



# Using bimetallic ZnCo-ZIFs as an efficient heterogeneous catalyst for the degradation of methyl blue in water in the presence of peroxymonosulfate ion

Huynh Thu Thao Nguyen<sup>1</sup> · Huynh Giao Dang<sup>1,2</sup> · Huynh Vu Thanh Luong<sup>1,2</sup> ·  
Luu Ngoc Hanh Cao<sup>1,2</sup> · Truong Ngoc Mai Ngo<sup>2</sup> · Tran Bao Nghi Pham<sup>1</sup> ·  
Trong Tuan Nguyen<sup>3</sup> · Quoc Chau Thanh Nguyen<sup>3</sup> · Minh Nhut Nguyen<sup>1</sup>

Received: 27 February 2022 / Accepted: 13 June 2022 / Published online: 18 June 2022  
© Akadémiai Kiadó, Budapest, Hungary 2022

## Abstract

ZnCo-ZIFs was successfully synthesized by a solvothermal method in methanol solvent at room conditions and determined physical–chemical properties by a series of characterization techniques. The catalytic activity of ZnCo-ZIFs on Methyl Blue (MB) degradation in the presence of peroxymonosulfate (PMS) was examined by variation of the effective factors including ZnCo-ZIFs dosage, mass ratio of ZnCo-ZIFs:PMS, temperature, reaction time and initial MB concentration. The result showed that MB was mostly degraded at initial MB concentration of 50 mg L<sup>-1</sup> with catalyst dosage of 50 mg L<sup>-1</sup> and ZnCo-ZIFs:PMS ratio of 1:3 at room temperature within 20 min of reaction. The main mechanism for dye degradation was the Fenton-like reaction via major active species SO<sub>4</sub>·<sup>-</sup> (sulfate free radical) generated from PMS by Co<sup>2+</sup> metal centers in the catalyst frameworks. The ZnCo-ZIFs showed highly efficient catalytic activity and stability compared to both homogeneous (cobalt salt, zinc salt and 2-methylimidazole) and heterogeneous (ZIF-67, ZIF-8, zeolite ZMS-5 and activated carbon) catalysts. The recyclability of the catalyst also showed an impressive result with 93.6% at the 5th recycle. To the best of our knowledge, ZnCo-ZIFs associated with PMS was first reported as a novel Fenton-like heterogeneous catalyst for MB degradation in water.

---

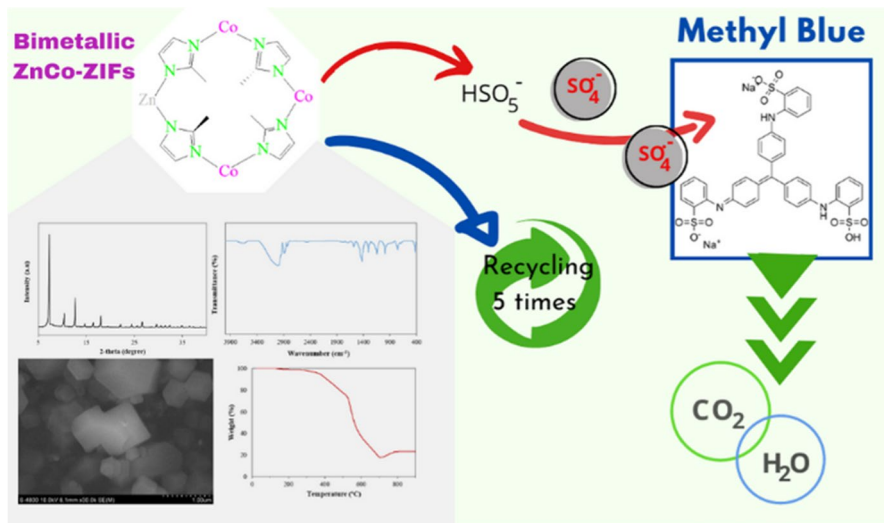
✉ Huynh Vu Thanh Luong  
lhvthanh@ctu.edu.vn

<sup>1</sup> Applied Chemical Engineering Lab, College of Engineering, Can Tho University, Can Tho 900000, Vietnam

<sup>2</sup> Department of Chemical Engineering, College of Engineering, Can Tho University, Can Tho 900000, Vietnam

<sup>3</sup> Department of Chemistry, College of Natural Sciences, Can Tho University, Can Tho 900000, Vietnam

## Graphical abstract



**Keywords** Bimetallic ZnCo-ZIFs · Heterogeneous catalyst · Peroxymonosulfate · Methyl Blue

## Introduction

Dye industry is considered as an important field in life, it has contributed a wide range of benefits for the social-economic development, such as clothes, rubber, plastics and biological dyeing, printing, etc. There are many types of dyes with more than 10,000 substances, categories based on either the chromophores or the principal applications [1]. It is reported that the annual production of dyes is  $7 \times 10^5$  tons throughout the world and the large amount of dye used also creates a huge excess released into the aqueous medium [2], which directly contaminates the environment, particularly water. In fact, according to a report from the World Bank, the textile dyeing sector contributes up to 20% of water pollution by releasing 13–45% of total colors used in dyeing into the environment through wastewater [3]. Most dyes are toxic, harmful for human health, which are extremely stable and cannot be broken down naturally [4, 5]. Among dyes, Methyl Blue (MB), an acid triphenylmethane dye, is often utilized for coloring collagen fiber and most suitable for dyeing silk and wool base materials [6], hence it is widely used in textiles. MB prevents sunlight from penetrating water, affecting the oxygen process, and so interfering with human and marine life [7]. The health and environmental effects caused by MB is highly disastrous because of its high thermal, photo stability and complex structure with many aromatic rings, which is difficult to remove from the

environment. Therefore, it is essential to remove MB in wastewater before discharging into the aquatic environment.

To remove MB in wastewater, many approaches are reported such as adsorption [8–11], photo-catalysis [12, 13], ion-exchange [14], membrane filtration [15]. Among these methods, advanced oxidation treatment presents more advantages. Fenton reaction, a typical technique of advanced oxidation processes (AOPs), is applied for persistent organic pollutants (POPs) removal with the advantages of high efficiency, no byproducts and low cost [16]. In Fenton-like reaction, a type of Fenton reaction, the high reactive species, i.e.,  $\cdot\text{OH}$ ,  $\text{SO}_4^{\cdot-}$ ,  $^1\text{O}_2$ , are produced from hydrogen peroxide  $\text{H}_2\text{O}_2$  or peroxymonosulfate (PMS) to accelerate the mineralization of POPs. In recent years, Fenton-like heterogeneous catalysts have been proposed as an attractive candidate for wastewater treatment because of its superiority such as environmental friendliness, energy efficiency [17] and recyclability [18]. The requirements of characteristics for heterogeneous Fenton-like catalyst must be highly porous natures, high stabilities, and large surface area [19]. One of the common catalysts is transition metals, which exhibit multiple oxidation states that suitable for the redox cycle which transforms the inactive species to the catalytically active species with specific oxidation state [20].

Zeolite imidazole frameworks (ZIFs) are formed via coordination bonding between metal ions and imidazolate ligands, and possess the similar structures to Zeolite, where metal ion and imidazole units substitutes the position of silicon and oxygen, respectively [21]. Some well-known properties of ZIFs materials are tunable structure, porosity, exception thermal, chemical and mechanical stability [22, 23], high surface area [24]. Bimetallic ZnCo-ZIFs is a new representative of ZIFs family, which contains two tetrahedral metal centers, Zn(II) and Co(II), randomly arranged in the frameworks. The combination of Zn and Co enhances the physical and chemical properties of ZnCo-ZIFs, increasing the pore volume compared to the monometallic ZIFs [25]. The recent development of bimetallic ZIFs attracted many researchers, concentrated on its arrangement and structures [26, 27], doping [28, 29] and applications [30–33]. One of the most attractive applications of bimetallic ZIFs is efficient heterogeneous catalysts. The synergy of bimetallic ZnCo-ZIFs and Fenton-like technology is a promising approach for MB removal in wastewater.

In this study, ZnCo-ZIFs is synthesized at ambient conditions and is behaved as a novel Fenton-like catalyst to activate PMS for MB degradation in aqueous solution under simulated laboratory conditions. The effect of different parameters, i.e. catalyst dosage, ZnCo-ZIFs:PMS mass ratio, reaction temperature, reaction time and initial MB concentration, on the degradation of MB catalyzed by ZnCo-ZIFs in the presence of PMS is conducted to elucidate the mechanism of the MB degradation process and the activity of the catalyst.

## Materials and methods

### Materials

2-Methylimidazole (2-MIm) ( $\text{C}_4\text{H}_6\text{N}_2$ , 99%) was purchased from Acros. Cobalt (II) nitrate hexahydrate ( $\text{Co}(\text{NO}_3)_2 \cdot 6\text{H}_2\text{O}$ , 99%), zinc (II) nitrate hexahydrate

( $\text{Zn}(\text{NO}_3)_2 \cdot 3\text{H}_2\text{O}$ , 99%), methanol ( $\text{CH}_3\text{OH}$ , 99.5%), NaOH 0.01 M, HCl 0.01 M and Methyl blue dye were purchased from Xilong Chemical Co., Ltd, China. Potassium peroxymonosulfate ( $\text{KHSO}_5 \cdot \text{KHSO}_4 \cdot \text{K}_2\text{SO}_4$ ) was purchased from Sigma Aldrich. All the reagents were used as received without further purification. Zeolite ZSM-5, activated carbon, ZIF-8 and ZIF-67 were used as heterogeneous catalysts.

## Synthesis of ZnCo-ZIFs

ZnCo-ZIFs were synthesized by the solvothermal method at room temperature in methanol solvent as reported in a previous study [34]. To this end,  $\text{Co}(\text{NO}_3)_2 \cdot 6\text{H}_2\text{O}$  (0.873 g, 3 mmol) and  $\text{Zn}(\text{NO}_3)_2 \cdot 6\text{H}_2\text{O}$  (0.297 g, 1 mmol) were separately dissolved in methanol (10 mL). Another solution was prepared by dissolving 2-MIm (2.6272 g, 32 mmol) in 30 mL methanol. Subsequently, zinc nitrate was added to the cobalt nitrate and magnetic stirring for 15 min to form a homogeneous mixture. Then, the material was synthesized via slow dripping of metal salts mixture into the 2-MIm solution under magnetic stirring, a purple suspension was formed and maintained at room temperature for 24 h. Thereafter, the purple solid was collected by centrifugation (6000 rpm, 15 min), washed with methanol ( $3 \times 10$  mL) and finally dried at  $60^\circ\text{C}$  for 12 h in the oven to obtain the ZnCo-ZIFs crystals.

## Characterizations of ZnCo-ZIFs

X-ray powder diffraction (PXRD) patterns were recorded using a Cu  $\text{K}_\alpha$  ( $\lambda = 1.5406 \text{ \AA}$ ) radiation source on a D8 Advance—Bruker powder diffractometer. The morphological features were examined by scanning electron microscope (SEM, Hitachi S4800). The specific surface areas of the samples were calculated using Brunauer–Emmett–Teller (BET) method. Fourier transform infrared spectroscopy (FT-IR) was obtained on a PerkinElmer instrument, with samples being dispersed on potassium bromide pallets. Atomic absorption spectroscopy (AAS) was used to analyze the metal elements and its contents in the ZnCo-ZIFs sample. Thermogravimetric analysis (TGA) was performed on a Setaram Labsys Evo instrument with the heating rate of  $10^\circ\text{C min}^{-1}$  in the  $\text{N}_2$  atmosphere.

## Determination of point of zero-charge (pHpzc)

pHpzc of ZnCo-ZIFs was determined by means of the pH drift method. The experiment set was designed as in the previous report [35]. The initial pH of 50 mL of 0.01 M NaCl solution was adjusted to pH values ranging from 2.0 – 12.0 by adding either HCl 0.01 M or NaOH 0.1 M solution. A 0.02 g of ZnCo-ZIFs was added and the suspension was shaken for 24 h at speed of 120 rpm. The solution after shaking was filtered and the final pH was determined. The pHpzc was the point where the final pH ( $\text{pH}_{\text{final}}$ ) and the initial pH ( $\text{pH}_{\text{initial}}$ ) are equal.

## Degradation of MB

ZnCo-ZIFs examined the catalytic ability for MB degradation. The deserved amount of ZnCo-ZIFs sample and PMS was dispersed into a 100 mL MB aqueous solution. The solution was heated to a deserved temperature and stirred for a deserved time at a speed of 400 rpm by a magnetic stirrer. After the reaction, the residual concentration of MB was measured by the UV–vis spectrophotometer at wavelength of 663 nm. Effective factors to the degradation process were observed including ZnCo-ZIFs dosage, ZnCo-ZIFs:PMS mass ratio, reaction time, reaction temperature and initial concentration of MB.

The degradation efficiency of MB was defined as following equation:

$$\text{Degradation efficiency(\%)} = \left( 1 - \frac{C_e}{C_0} \right) \times 100 \quad (1)$$

Here  $C_0$  is the initial concentration of MB ( $\text{mg L}^{-1}$ ),  $C_e$  is the residual concentration of MB ( $\text{mg L}^{-1}$ ).

The using of other oxidants at optimal experiment parameters was examined to compare the degradation efficiency of different oxidant agents. The residual concentration of MB after reaction will be measured by the UV–vis spectrophotometer at wavelength of 663 nm.

## Reusability of ZnCo-ZIFs

The reusability of ZnCo-ZIFs catalyst in removal of MB was evaluated by conducting repeated experiments. In detail, the ZnCo-ZIFs used in the optimal condition experiment for MB removal were recovered by filtration, washed several times with methanol, then dried at 60 °C overnight before reusing as the catalyst for the next cycle. This procedure was repeated several times until the degradation efficiency reduced remarkably and the recovered catalyst at the last run was analyzed by PXRD and FT-IR to evaluate the structural stability.

## Results and discussion

### Synthesis of ZnCo-ZIFs

The ZnCo-ZIFs was successfully prepared by solvothermal method in methanol at room conditions in 24 h, appeared in form of purple powder, then collected by centrifugation, washed with methanol, and dried at 60 °C. The synthesis efficiency was determined of 53.4% (0.45 g of ZnCo-ZIFs), calculated by the molar of Zinc salt. Then, the synthesized ZnCo-ZIFs catalyst is structurally and chemically analyzed by characterization methods, namely PXRD, FT-IR, SEM, TGA, AAS, BET.

The PXRD spectrum is shown in Fig. 1, which strongly proved the formation of crystalline ZnCo-ZIFs material with the specific peaks corresponding to the

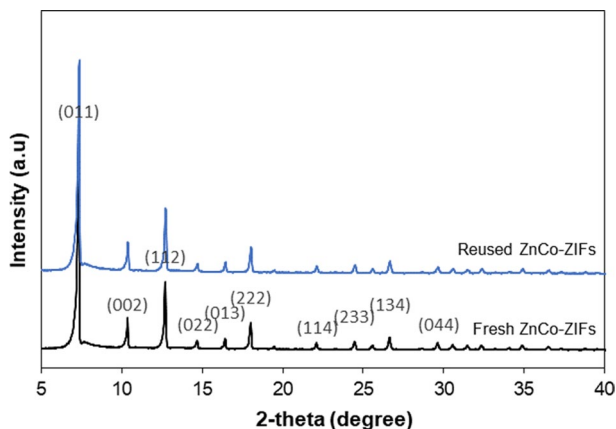


Fig. 1 PXRD of ZnCo-ZIFs

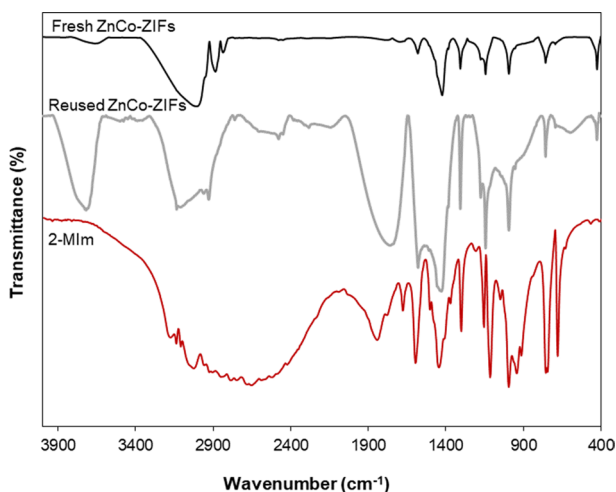


Fig. 2 FT-IR of fresh ZnCo-ZIFs, 2-MIm and reused ZnCo-ZIFs

different lattices of the crystal, were in excellent agreement with previous report from Zhou et al. (2017) [36]. Specifically, there were featured peaks at  $2\theta$  of 7.2, 10.3, 12.7, 14.6, 16.4, 18 degree corresponding to the surface lattices of (011), (002), (112), (002), (013) and (222). This proved the polyhedron of crystal structure. The sharp and high intensity peaks at  $2\theta$  of 7.2 and 12.6 were indicated as evidence for the obtaining of highly crystalline material [36]. The FT-IR result in Fig. 2 shows the featured functional groups presence in the materials. The peak at  $425.06\text{ cm}^{-1}$  which was the stretching mode of C atoms in ligands and metal centers, proved the successful formation of the framework structure. Other peaks from  $600\text{--}1500\text{ cm}^{-1}$  were stretching oscillations of 2-MIm ligands. A small

adsorption band at  $3031.34\text{ cm}^{-1}$  was the result of deprotonation process of the N–H groups of the 2-MIm ligands upon coordination with metal ions, from the broad band from  $3400$  to  $2200\text{ cm}^{-1}$  was found as the N–H–N bond established from two 2-MIm ligands [36].

The surface shape of ZnCo-ZIFs was provided with SEM images (Supplementary Information), where ZnCo-ZIFs presented the crystalline possessing a rhombic dodecahedron shape and smooth surface. These results were similar to other reported materials on the structure of ZIF-8 and ZIF-67 [27]. In addition, ZnCo-ZIFs was stable at high temperatures up to  $400\text{ }^{\circ}\text{C}$ , measured by TGA (Supplementary Information). The weight loss started from about  $100$ – $250\text{ }^{\circ}\text{C}$ , which was mainly the release of MeOH, water, air and excess 2-MIm ligands. From  $400\text{ }^{\circ}\text{C}$  up to  $700\text{ }^{\circ}\text{C}$ , there was a drop down of weight due to the collapse of organic linkers and the structural breakdown. By using AAS, the amount of two metals Co and Zn are determined at  $196.2\text{ }\mu\text{g g}^{-1}$  and  $61.6\text{ }\mu\text{g g}^{-1}$ , respectively. These amounts were well matched with the molar ratio of Cobalt salt and Zinc salt used in the synthesis procedure, which was 1:3. This result strongly proved the successfully coordinated bonding between metal ions and organic linkers in the frameworks. The information of porosity and surface area of the material was also determined by BET, with the surface area was  $1191.6\text{ m}^2\text{ g}^{-1}$  and pore size was  $16.4\text{ }\text{\AA}$ . The pH<sub>pzc</sub> of ZnCo-ZIF was determined as around 9 (Supplementary Information). This value was in good agreement with pH<sub>pzc</sub> of ZIF-67 (8.7) [37] and ZIF-8 (9.5) [36]. The stability of ZnCo-ZIFs was also defined through this test that ZnCo-ZIFs framework structure collapsed at pH solutions lower than 3 and higher than 12.

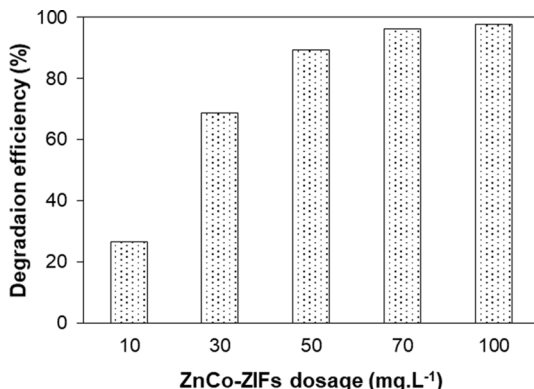
### Catalytic activity of ZnCo-ZIFs on MB degradation

The catalytic potential of ZnCo-ZIFs was investigated by the degradation of MB process, which depended on various influenced factors such as catalyst dosage, PMS amount, reaction time, reaction temperature, dye concentration.

It is important to investigate the ZnCo-ZIFs dosage in the MB degradation, because the amount of catalyst is used to activate PMS and produce  $\text{SO}_4^{\cdot-}$ , which is a main oxidation agent to degrade MB. In order to study the effect of ZnCo-ZIFs, the experiment set was conducted with the catalyst dosage increased from  $10\text{ mg L}^{-1}$  to  $100\text{ mg L}^{-1}$  and the result is shown in Fig. 3.

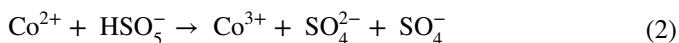
Generally, the amount of ZnCo-ZIFs is proportional to the MB degradation efficiency. The activity of Zn(II) and Co(II) accelerated the decomposition of PMS to produce  $\text{SO}_4^{\cdot-}$  free radical. This radical is the main factor attacked to the major links of the dye structure to break it down, leading to the discoloring of dye. The degradation efficiency markedly increased from 26.4% to 68.8% and then 89.4% with increasing of the catalyst dosage from  $10\text{ mg L}^{-1}$  to  $30\text{ mg L}^{-1}$  and  $50\text{ mg L}^{-1}$ . When the catalyst dosage increased to a higher amount, the efficiency just rose by 6.9% from catalyst dosage of  $50\text{ mg L}^{-1}$  to  $70\text{ mg L}^{-1}$  and by 1.5% from catalyst dosage of  $70\text{ mg L}^{-1}$  to  $100\text{ mg L}^{-1}$ . Hence, the optimal ZnCo-ZIFs catalyst dosage for MB removal was chosen at  $50\text{ mg L}^{-1}$  in the following experiments.

**Fig. 3** Effect of catalyst dosage on the degradation of MB catalyzed by ZnCo-ZIFs in the presence of PMS (Initial pH 3.0, ZnCo-ZIFs:PMS mass ratio = 1:2, reaction temperature = 30 °C, contact time = 30 min, MB concentration = 50 ppm)



The oxidation agent is also a critical factor in the Fenton-like reaction because it is directly related to the dye degradation. The PMS amount was studied as a ratio with catalyst dosage and the result is presented in Fig. 4.

The result showed that the PMS amount had an influence on the MB. With the mass ratio of ZnCo-ZIFs:PMS increased from 1:1 to 1:2 and 1:3, the MB degradation increased from 54.1% to 89.4% and 99.2%. At higher ratios, 1:4 and 1:5, the degradation efficiency changed insignificantly and kept constant at 99.9%. The decomposition of PMS activated by heterogeneous catalyst ZnCo-ZIFs led to the generation of sulfate radical  $\text{SO}_4^{\cdot-}$ , which mainly contributed to the degradation of dyes, as presented in equation [38] Eq. (2).



In Fig. 4, at a mass ratio of 1:3, the dye degradation process started to reach equilibrium, hence, this value was chosen as the optimal ratio of ZnCo-ZIFs:PMS, which the mass of PMS used was 0.015 g.

Temperature is a relatedly affected factor of the reaction because the change of temperature leads to the change of entropy and kinetic reaction. The temperature in this work was studied by experiment set at a temperature range from room

**Fig. 4** Effect of ZnCo-ZIFs:PMS mass ratio on the degradation of MB catalyzed by ZnCo-ZIFs in the presence of PMS (Initial pH 3.0, ZnCo-ZIFs dosage = 50 mg L<sup>-1</sup>, reaction temperature = 30 °C, contact time = 30 min, MB concentration = 50 ppm)

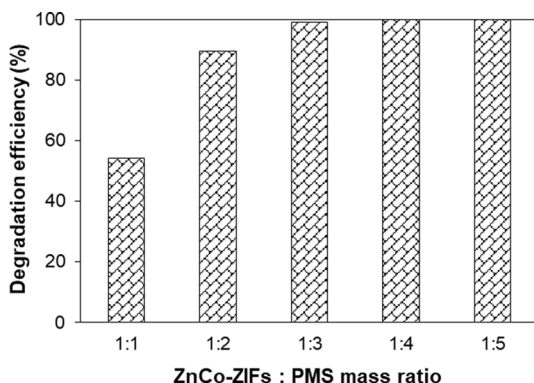




**Fig. 5** Effect of reaction temperature on the degradation of MB catalyzed by ZnCo-ZIFs in the presence of PMS (Initial pH 3.0, ZnCo-ZIFs dosage = 50 mg L<sup>-1</sup>, ZnCo-ZIFs:PMS mass ratio = 1:3, contact time = 30 min, MB concentration = 50 ppm)

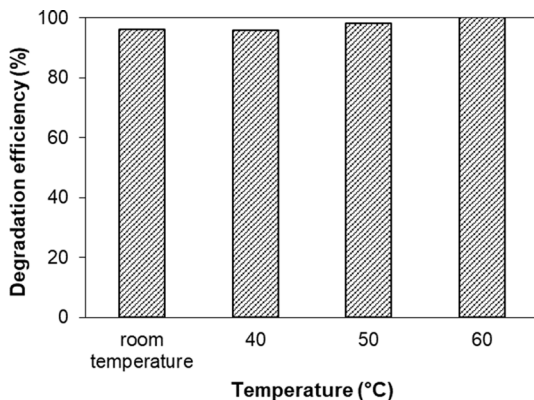
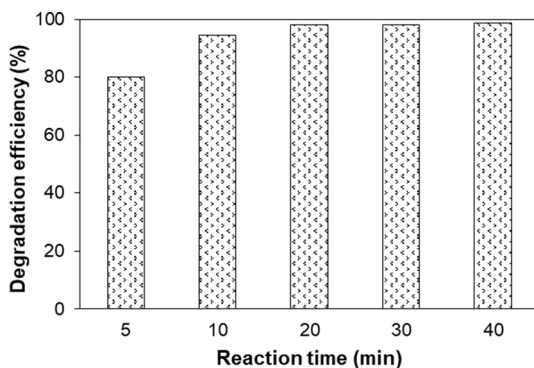


**Fig. 6** Effect of reaction time on the degradation of MB catalyzed by ZnCo-ZIFs in the presence of PMS (Initial pH 3.0, ZnCo-ZIFs dosage = 50 mg L<sup>-1</sup>, ZnCo-ZIFs:PMS mass ratio = 1:3, reaction temperature = 30 °C, MB concentration = 50 ppm)



temperature to 60 °C. The effect of temperature to MB degradation efficiency is presented in Fig. 5.

As can be seen from Fig. 5, there was an obvious tendency which showed the effect of temperature to the degradation process. The more the temperature increased, the higher the degradation efficiency was. In detail, at room temperature, the degradation efficiency was 96.1%, and this yield increased to 98% and 100% with increasing temperature to 50 °C and 60 °C, respectively. However, it is obvious that temperature does not have much influence on the degradation process, because the increase of degradation efficiency was insignificant as the temperature increased by 10 °C for each interval. Hence, in order to be simple, effective and convenient, the temperature chosen for following experiments was room temperature.

Contact time is a factor directly related to the reaction rate constant; hence it is required to investigate the reaction time. The investigation of time on degradation efficiency was performed by conducting experiments at different time intervals from 5 to 40 min. The result is shown in Fig. 6.

The degradation efficiency was proportional to longer time; the longer time is, the higher dye degradation efficiency obtains. Within the first 5 min, the

**Fig. 7** Effect of initial MB concentration on the degradation of MB catalyzed by ZnCo-ZIFs in the presence of PMS (Initial pH 3.0, ZnCo-ZIFs dosage = 50 mg L<sup>-1</sup>, ZnCo-ZIFs:PMS mass ratio = 1:3, reaction temperature = 30 °C, contact time = 20 min)

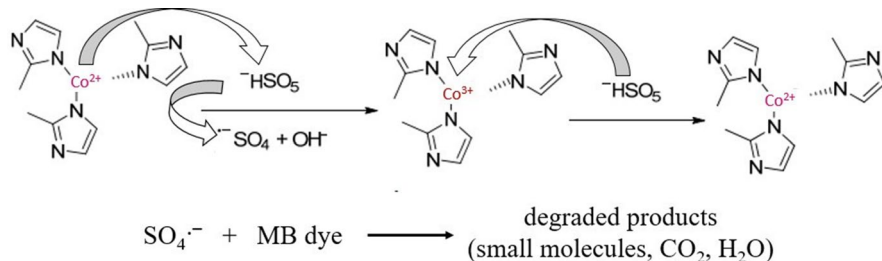
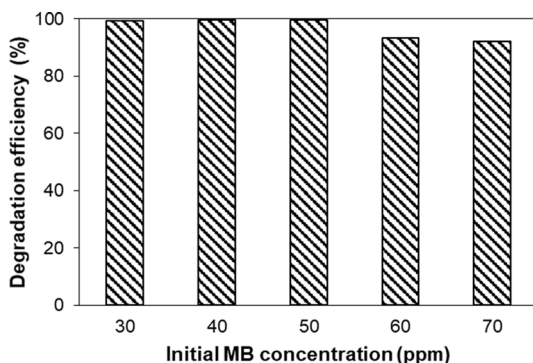


**Fig. 8** Mechanism of MB degradation catalyzed by ZnCo-ZIFs in the presence of PMS, following Fenton-like reaction

degradation efficiency got 80.0% and then increased to 94.4% at 10 min. After that, the removal process reached equilibrium yield with 98.1% at 20 min and 30 min, and slightly increased to 98.5% at 50 min. Therefore, 20 min could be considered as the optimal reaction time.

In wastewater, the dye concentration varies, therefore, the initial dye concentration must be studied. The initial MB concentration in this work was modified from 30 to 70 ppm.

The result presented in Fig. 7 shows the effect of initial MB concentration from 30 to 70 ppm. The MB degradation efficiency remained unchanged at about 99% with the concentration varied from 30 to 50 ppm, and remarkably downed to 93.4% at 60 ppm. At high concentration, there were more dye molecules, and it required more oxidant and free radicals to degrade all dyes, which caused the cost effectiveness. Hence, 50 ppm was chosen as the optimal MB initial concentration.

The mechanism of MB mineralization could be suggested by a Fenton-like process and illustrated as in Fig. 8.

In the MB degradation process, there were two stages proposed. The first stage was the decomposition of PMS under the activation of Co(II) in ZnCo-ZIFs. The interaction between Co(II) and PMS induced the  $\text{SO}_4^{\cdot-}$  radicals, while Co(II) transferred into Co(III). The catalyst is converted by the reaction of  $\text{HSO}_5^-$  anion and Co(III) to re-form Co(II) and at the same time generate more free radicals  $\text{SO}_4^{\cdot-}$ . In the second stage, the  $\text{SO}_4^{\cdot-}$  species attacked to the MB molecules, broke down the structure of dye

to turn the dye into harmless matters. Finally, after many intermediate reactions, the degraded products were proposed as  $\text{CO}_2$ ,  $\text{H}_2\text{O}$ , and other small and harmless inorganic molecules.

In addition, to emphasize the catalytic ability of ZnCo-ZIFs, the catalytic activity of ZnCo-ZIFs in the presence of PMS was also compared with other oxidation agents at the optimum experiment parameters, including 0.005 g ZnCo-ZIFs,  $0.0488 \times 10^{-3}$  mol of oxidants (equal to 0.015 g of PMS), 20 min in room temperature and MB concentration of 50 ppm. The result was shown in Table 1.

In Table 1, degradation efficiency between various oxidation conditions was presented and an apparently distinctive difference between those experiments was observed. This result emphasized the Fenton-like catalytic role of ZnCo-ZIFs, the strong oxidation agent PMS and the synergetic effect by the combination of bimetallic ZnCo-ZIFs/PMS systems. Detailed, the degradation efficiency of ZnCo-ZIFs associated with PMS was highest as desirable, while alone PMS also performed but the degradation efficiency was moderate, just 63.1%. Another oxidizing agent,  $\text{H}_2\text{O}_2$  was also used, and the efficiency was extremely low, only 0.85%, and the activation  $\text{H}_2\text{O}_2$  by ZnCo-ZIFs did not react as high efficiency as proposed as well. The reason could be due to the different strength of PMS and  $\text{H}_2\text{O}_2$  and the free radicals generated by each oxidant, which  $\text{SO}_4^{\cdot-}$  is stronger than  $\cdot\text{OH}$  (standard reduction potential: 2.5–3.1 V vs. 1.8–2.7 V). The ZnCo-ZIFs alone also presented the removal efficiency on MB; however, this might be because of the adsorption process and the slight photo-catalysis, and the removal was ineffective.

The homogeneous catalysts were used to compare the catalytic capacity with ZnCo-ZIFs, including cobalt nitrate salt, zinc nitrate salt and 2-MIm, which were the precursors to synthesize ZnCo-ZIFs. Some well-known heterogeneous catalysts, namely activated carbon, zeolite, ZIF-8 and ZIF-67, were also studied in the MB removal process under the same conditions.

As shown in Fig. 9, the removal of MB was high with ZnCo-ZIFs and cobalt salt, and worse with zinc salt and 2-MIm. The high degradation efficiency achieved by cobalt salt could be due to the dissociation of Co(II) into solution and then Co(II) ions active PMS for the degradation process. The effect achieved when using 2-MIm and Zinc salt could be explained by the reaction conditions, under stirring speed and the decomposition of PMS under visible light and stirring [39].



**Table 1** Comparison of ZnCo-ZIFs activated PMS and other oxidation on the degradation of MB catalyzed by ZnCo-ZIFs in the presence of PMS

Oxidation conditions			Degradation efficiency (%)
ZnCo-ZIFs (g)	PMS (g)	$\text{H}_2\text{O}_2$ (mL)	
0.005	0.015	0	97.4
0.005	0	0.001	6.68
0	0.015	0	63.1
0	0	0.001	0.85
0.005	0	0	7.62

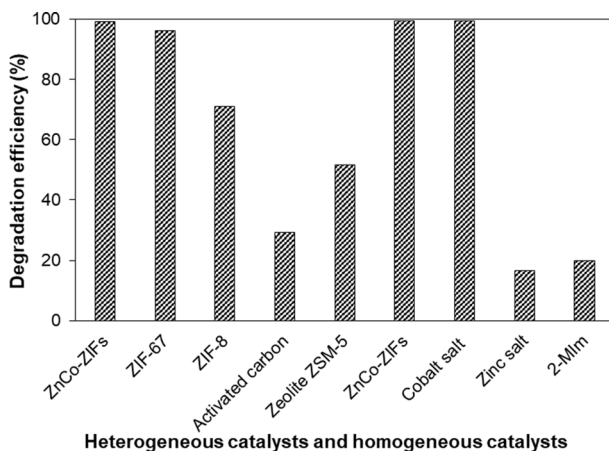
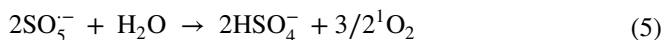
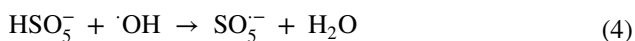


**Fig. 9** Comparison of homogeneous catalysts and heterogeneous catalysts on the degradation of MB catalyzed by ZnCo-ZIFs in the presence of PMS (Initial pH 3.0, ZnCo-ZIFs dosage = 50 mg L<sup>-1</sup>, catalyst:PMS mass ratio = 1:3, reaction temperature = 30 °C, contact time = 20 min, MB concentration = 50 ppm)



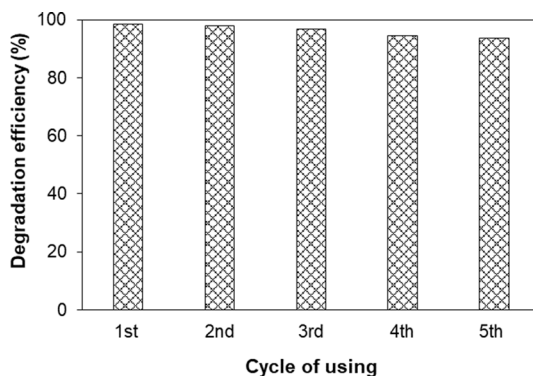
In heterogeneous catalysts comparison, the ZnCo-ZIFs also showed an exceptional efficiency, which was 99.3%. ZIF-67 and ZIF-8 reached a degradation efficiency of 96.2% and 71.1%, respectively. The metal centers in those ZIFs acted on PMS and that could degrade dye molecules. The degradation efficiency was low by using zeolite and activated carbon, because the removal process occurred mainly throughout the adsorption to the porous structure of these materials.

### Reusability of ZnCo-ZIFs catalyst

The important property of heterogeneous catalysts is the reusability. The repeating experiment set was conducted to evaluate the using cycles of ZnCo-ZIFs and the results are shown in Fig. 10.

After five times of using, the dye degradation efficiency still maintained at above 90% and decreased very little after each cycle. The degradation efficiency slightly decreased from 98.5% to 98% at the first two cycles, then dropped down to 96.6%, 94.5% and 93.6% at the next cycles. The reason for high degradation efficiency of reused ZnCo-ZIFs might be due to the heterogeneous metal ions Co(II), which linked structurally with the frameworks and did not lose after many times of using. Hence, it can be confirmed that ZnCo-ZIFs possessed the reusability for MB

**Fig. 10** The degradation efficiency of MB catalyzed by ZnCo-ZIFs in the presence of PMS at different recycles (Initial pH 3.0, ZnCo-ZIFs dosage = 50 mg L<sup>-1</sup>, ZnCo-ZIFs:PMS mass ratio = 1:3, reaction temperature = 30 °C, contact time = 20 min, MB concentration = 50 ppm)



degradation in aqueous solution. In addition, the structural stability of ZnCo-ZIFs catalyst was examined by PXRD and FT-IR analysis.

The crystal structure of the material was provided with PXRD patterns. The result from Fig. 1 shows the completed match of the fresh and reused material, there was almost no change in the XRD patterns of the reused material compared to the fresh one. The intact specific sharp peaks at  $2\theta$  of 7.2 and 12.6 degree corresponding to the lattice (011) and (112) proved the highly crystalline structure of ZnCo-ZIFs after 5 times of using. To assess the functional groups and featured bonding in the reused materials, the FT-IR of reused ZnCo-ZIFs was assigned and compared with the fresh material (Fig. 2). The FT-IR spectrum of reused materials presented the similar peaks from 3900 cm<sup>-1</sup> to 1500 cm<sup>-1</sup>, which originally was the oscillations from 2-Mim ligands, with the broad transmittance and noise. The featured peaks of C-metals bonding moved a little from 425.06 cm<sup>-1</sup> to 425.87 cm<sup>-1</sup>, proving the stable featured bonding of metal ions and organic linkers. There were two small peaks at 2200–2500 cm<sup>-1</sup>, where was measuredly C≡N stretching. Another new broad peak appeared at 1700–1800 cm<sup>-1</sup> was assigned as the stretching oscillation of carboxylic acid C=O, which could be one of the small molecules degraded products. These peaks could demonstrate that the immediate and final products of MB breakdown process were adsorbed in the pores of the catalyst, causing the decrease in degradation efficiency after five cycles.

## Conclusions

The bimetallic ZnCo-ZIFs was successfully synthesized and applied as a heterogeneous catalyst to activate PMS for MB removal via Fenton-like reaction. The properties of ZnCo-ZIFs were illuminated by characterization techniques, i.e., PXRD, FT-IR, TGA, BET, SEM, AAS. The MB degradation optimal condition was confirmed with 50 mg L<sup>-1</sup> of catalyst dosage, initial MB concentration of 50 mg L<sup>-1</sup> with ZnCo-ZIFs:PMS mass ratio of 1:3 at room temperature within 20 min. The reusability of ZnCo-ZIFs was also confirmed that it could perform high catalytic efficiency with more than 90% after 5 times of recycling. The stepwise mechanism

and intermediate products of the MB degradation process should be investigated by HPLC technique for further understanding. Finally, ZnCo-ZIFs, with its exceptional properties, is a potential catalyst for contaminants degradation in wastewater treatment.

**Supplementary Information** The online version contains supplementary material available at <https://doi.org/10.1007/s11144-022-02240-8>.

**Funding** The authors did not receive support from any organization for the submitted work.

## Declarations

**Conflict of interest** The authors have no relevant financial or non-financial interests to disclose.

## References

1. Gregory P (2007). In: Hunger K (ed) Industrial dyes: chemistry, properties, applications. John Wiley & Sons, Weinheim
2. Hussain S, Kamran M, Khan S, Shaheen K, Shah Z, Suo H, Ghani U (2021) Adsorption, kinetics and thermodynamics studies of methyl orange dye sequestration through chitosan composites films. *Int J of biological macromol* 168:383–394
3. Shafiq F, Siddique A, Pervez M, Hassan M, Naddeo V, Cai Y, Hou A, Xie K, Khan M, Kim I (2021) Extraction of natural dye from aerial parts of argy wormwood based on optimized Taguchi approach and functional finishing of cotton fabric. *Mater* 14(19):5850–5869
4. Liu M, Wang Z (2021) Adsorption performance of reactive red 2BF onto magnetic  $Zn_{0.3}Cu_{0.7}Fe_2O_4$  nanoparticles. *Mater Res Express* 8(2):025014–025025
5. Chen J, Wang Z, Lv Z (2021) Adsorption of reactive red 2BF onto  $Ni_{0.3}Co_{0.2}Zn_{0.5}Fe_2O_4$  nanoparticles fabricated via the ethanol solution of nitrate combustion process. *Mater Res Express* 8(1):015006–015017
6. Oyewo O, Nevondo N, Onwudiwe D, Onyango M (2021) Photocatalytic degradation of methyl blue in water using sawdust-derived cellulose nanocrystals-metal oxide nanocomposite. *J of Inorg and Organomet Polym and Mater* 31(6):2542–2552
7. Shen T, Liu G, Wei L, Zhu Y, Sun S (2019) Construction of ZnS nanoparticles@porous  $Cu_3SnS_4$  P-N heterojunction for simulated natural sunlight degradation of methyl blue. *Mater Lett* 253:446–449
8. Arora C, Kumar P, Soni S, Mittal J, Mittal A, Singh B (2020) Efficient removal of malachite green dye from aqueous solution using Curcuma caesia based activated carbon. *Desalin Water Treat* 195:341–352
9. Zhang Z, Zhang J, Liu J, Xiong Z, Chen X (2016) Selective and competitive adsorption of azo dyes on the metal–organic framework ZIF-67. *Water Air Soil Pollut* 227(12):471–483
10. Santoso E, Ediati R, Istiqomah Z, Sulistiono D, Nugraha R, Kusumawati Y, Bahruji H, Prasetyoko D (2021) Facile synthesis of ZIF-8 nanoparticles using polar acetic acid solvent for enhanced adsorption of methylene blue. *Microporous and Mesoporous Mater* 310:110620–110630
11. Feng Y, Li Y, Xu M, Liu S, Yao J (2016) Fast adsorption of methyl blue on zeolitic imidazolate framework-8 and its adsorption mechanism. *RSC Adv* 6(111):109608–109612
12. Tanaka K, Padermpole K, Hisanaga T (2000) Photocatalytic degradation of commercial azo dyes. *Water Res* 34(1):327–333
13. Bhuvaneswari K, Palanisamy G, Pazhanivel T, Maiyalagan T, Shanmugam P, Grace A (2021) In-situ development of metal organic frameworks assisted ZnMgAl layered triple hydroxide 2D/2D hybrid as an efficient photocatalyst for organic dye degradation. *Chemosphere* 270:128616–128626
14. Wawrzkiwicz M, Hubicki Z (2016) Anion exchange resins of tri-n-butyl ammonium functional groups for dye baths and textile wastewater treatment. *Solvent Extr and Ion Exch* 34(6):558–575
15. Donkadokula N, Kola A, Naz I, Saroj D (2020) A review on advanced physico-chemical and biological textile dye wastewater treatment techniques. *Rev in environ sci and biotechnol* 25:1–8

16. González J, Gamallo M, Conde J, Vargas-Osorio Z, Vázquez C, Piñeiro Y, Rivas J, Feijoo G, Moreira M (2021) Exploiting the potential of supported magnetic nanomaterials as Fenton-like catalysts for environmental applications. *Nanomater* 11(11):2902–2918
17. Liang D, Li N, An J, Ma J, Wu Y, Liu H (2021) Fenton-based technologies as efficient advanced oxidation processes for microcystin-LR degradation. *Sci Total Environ* 753:141809–141826
18. Zuo S, Jin X, Wang X, Lu Y, Zhu Q, Wang J, Liu W, Du Y, Wang J (2021) Sandwich structure stabilized atomic Fe catalyst for highly efficient Fenton-like reaction at all pH values. *Appl Catal B: Environ* 282:119551–119558
19. Wang N, Zheng T, Zhang G, Wang P (2016) A review on Fenton-like processes for organic wastewater treatment. *J of Environ Chem Eng* 4(1):762–787
20. Bokare A, Choi W (2014) Review of iron-free Fenton-like systems for activating H<sub>2</sub>O<sub>2</sub> in advanced oxidation processes. *J of Hazard Mater* 275:121–135
21. Chen B, Yang Z, Zhu Y, Xia Y (2014) Zeolitic imidazolate framework materials: recent progress in synthesis and applications. *J of Mater Chem A* 2(40):16811–16831
22. Park K, Ni Z, Côté A, Choi J, Huang R, Uribe-Romo F, Chae H, O’Keeffe M, Yaghi O (2006) Exceptional chemical and thermal stability of zeolitic imidazolate frameworks. *Proc Natl Acad Sci* 103(27):10186–10191
23. Tan J, Bennett T, Cheetham A (2010) Chemical structure, network topology, and porosity effects on the mechanical properties of Zeolitic Imidazolate Frameworks. *Proc Natl Acad Sci* 107(22):9938–9943
24. Chen Y, Wang C, Wu Z, Xiong Y, Xu Q, Yu S, Jiang H (2015) From bimetallic metal-organic framework to porous carbon: high surface area and multicomponent active dopants for excellent electrocatalysis. *Adv Mater* 27(34):5010–5016
25. Kaur G, Rai R, Tyagi D, Yao X, Li P, Yang X, Zhao Y, Xu Q, Singh S (2016) Room-temperature synthesis of bimetallic Co–Zn based zeolitic imidazolate frameworks in water for enhanced CO<sub>2</sub> and H<sub>2</sub> uptakes. *J of Mater Chem A* 4(39):14932–14938
26. Imawaka K, Sugita M, Takewaki T (2019) Tanaka S (2019) Mechanochemical synthesis of bimetallic CoZn-ZIFs with sodalite structure. *Polyhedron* 158:290–295
27. Saliba D, Ammar M, Rammal M, Al-Ghoul M, Hmadeh M (2018) Crystal growth of ZIF-8, ZIF-67, and their mixed-metal derivatives. *J of the Am Chem Soc* 140(5):1812–1823
28. Yao M, Ye Y, Chen H, Zhang X (2020) Porous carbon supported Pd as catalysts for boosting formic acid dehydrogenation. *Int J of Hydrog Energy* 45(35):17398–17409
29. Dong S, Li T, Zhang Z, Sun M, An L (2019) Improving electrical contact properties of carbon nanotubes by Co doping using metal-organic framework as template. *Mater Lett* 253:420–423
30. Chaemchuen S, Dai Q, Wang J, Zhu C, Klomkliang N, Yuan Y, Cheng C, Elkadi M, Luo Z, Verpoort F (2021) Enhancing catalytic activity via metal tuning of zeolitic imidazole frameworks for ring opening polymerization of L-lactide. *Appl Catal A: General* 624:118319–118335
31. Lee S, Choi S (2017) Bimetallic zeolitic imidazolate frameworks for symmetric electrical double-layer supercapacitors with aqueous electrolytes. *Mater Lett* 207:129–132
32. Nandigama S, Bheeram V, Mukkamala S (2019) Rapid synthesis of mono/bimetallic (Zn/Co/Zn–Co) zeolitic imidazolate frameworks at room temperature and evolution of their CO<sub>2</sub> uptake capacity. *Environ Chem Lett* 17(1):447–454
33. Han X, Ling X, Wang Y, Ma T, Zhong C, Hu W, Deng Y (2019) Generation of nanoparticle, atomic-cluster, and single-atom cobalt catalysts from zeolitic imidazole frameworks by spatial isolation and their use in zinc–air batteries. *Angew Chem* 131(16):5413–5418
34. Giao D, Le Thu TA, Nguyen THT, Tan HNT, Doan TVH, Van Toan P (2020) Facile synthesis of bimetallic ZnCo-ZIFs and Ag nanoparticles loading on ZnCo-ZIFs (Ag/ZnCo-ZIFs). *Can Tho University Journal of Science* 12(3):47–53
35. Jing H, Wang C, Zhang Y, Wang P, Li R (2014) Photocatalytic degradation of methylene blue in ZIF-8. *Rsc Adv* 4(97):54454–54462
36. Zhou K, Mousavi B, Luo Z, Phatanasri S, Chaemchuen S, Verpoort F (2017) Characterization and properties of Zn/Co zeolitic imidazolate frameworks vs. ZIF-8 and ZIF-67. *J of Mater Chem A* 5(3):952–957
37. Mostafazadeh N, Ghoreyshi AA, Pirzadeh K (2018) Optimization of solvothermally synthesized ZIF-67 metal organic framework and its application for Cr (VI) adsorption from aqueous solution. *Iranian Journal of Chemical Engineering* 15(4):27–47
38. Song X, Shao X, Dai L, Fan D, Ren X, Sun X, Luo C, Wei Q (2020) Triple amplification of 3, 4, 9, 10-Perylenetetra-carboxylic acid by Co<sup>2+</sup>-based metal-organic frameworks and silver-cysteine

- and its potential application for ultrasensitive assay of procalcitonin. *ACS Appl Mater & interfaces* 12(8):9098–9106
39. Chen F, Huang G, Yao F, Yang Q, Zheng Y, Zhao Q, Yu H (2020) Catalytic degradation of ciprofloxacin by a visible-light-assisted peroxymonosulfate activation system: performance and mechanism. *Water Res* 173:115559–115571

**Publisher's Note** Springer Nature remains neutral with regard to jurisdictional claims in published maps and institutional affiliations.